Climate-induced decrease in biomass flow in marine food webs may severely affect predators and ecosystem production

Running title: Climate-induced decrease in biomass flow

Hubert **du Pontavice**[a, b, c *], Didier Gascuel[a], Gabriel Reygondeau[d], Charles Stock[e], William W. L. Cheung[b, d]

[a] ESE, Ecology and Ecosystems Health, Institut Agro, Inrae, Rennes, France,

[b] Nippon Foundation-Nereus Program, Institute for the Oceans and Fisheries, University of British Columbia, Vancouver, British Columbia, Canada

[c] Princeton University, Atmospheric and Oceanic Sciences program, Princeton, New Jersey, USA

[d] Institute for the Oceans and Fisheries, University of British Columbia, Vancouver, British Columbia, Canada

[e] Geophysical Fluid Dynamics Laboratory, National Oceanic and Atmospheric Administration, Princeton University, Princeton, New Jersey, USA

* Contact author, E-mail: hubert.dupontavice@gmail.com, Phone number: +33 783-361-992

Keywords

Marine Food Web, Climate Change, Trophic Ecology, Ecosystem Modelling, Biomass Flow, Trophic Structure, EcoTroph

Abstract

Climate change impacts on marine life in the world ocean are expected to accelerate over the 21st century, affecting the structure and functioning of food webs. We analyzed a key aspect of this issue, focusing on the impact of changes in biomass flow within marine food webs and the resulting effects on ecosystem biomass and production. We used a modeling framework based on a parsimonious quasi-physical representation of biomass flow through the food web, to explore the future of marine consumer biomass and production at the global scale over the 21st century. Biomass flow is determined by three climate-related factors: primary production entering the food web, trophic transfer efficiency describing losses in biomass transfers from one trophic level to the next, and flow kinetic measuring the speed of biomass transfers within the food web. Using climate projections of three Earth system models, we calculated biomass and production at each trophic level on a 1° latitude x 1° longitude grid of the global ocean under two greenhouse gas emissions scenarios. We show that the alterations of the trophic functioning of marine ecosystems, mainly driven by faster and less efficient biomass transfers and decreasing primary production, would lead to a projected decline in total consumer biomass by 18.5% by 2090–2099 relative to 1986–2005 under the "no mitigation policy" scenario. The projected decrease in transfer efficiency is expected to amplify impacts at higher trophic levels, leading to a 21.3% decrease in abundance of predators and thus to a change in the overall trophic structure of marine ecosystems. Marine animal's production is also projected to decline but to a lesser extent than biomass. Our study highlights that the temporal and spatial projected changes in biomass and production would imply direct repercussions on the future of world fisheries and beyond all services provided by Ocean.

1. INTRODUCTION

Human-induced climate change is already impacting ocean ecosystems by driving major changes in their physical and chemical properties and the impacts are expected to intensify over the 21st century particularly under insufficient carbon mitigation (Bindoff et al., 2019; IPCC, 2014). One of the marine ecosystem components that are impacted by changes in ocean properties is net primary production (NPP) that plays an essential role in fueling energy and biomass up marine food webs. Total NPP of the ocean is projected to decrease over the course of the 21st century (Bopp et al., 2013; Cabré et al., 2015; Laufkötter et al., 2015). Regionally, NPP is projected to decrease in the low-latitude regions and to increase at high latitude, mainly due to the stratification-induced exacerbation of nutrient limitation at low latitude and to an alleviation of light limitation as a result of loss of sea ice at high latitude (Bopp et al., 2013; Cabré et al., 2015; Laufkötter et al., 2015).

These projected changes in NPP as well as the changing ocean conditions are impacting the physiology and biogeography of marine organisms with cascading effects on ecosystem structure and functions (Bindoff et al., 2019). Ocean warming, deoxygenation and ocean acidification alter the physiology and fitness of marine organisms (Pörtner et al., 2017; Pörtner & Farrell, 2008; Pörtner & Peck, 2010), causing shifts in species distribution (Jones & Cheung, 2015; Pinsky et al., 2013; Poloczanska et al., 2013), phenology (Asch et al., 2019; Burrows et al., 2014) and changes in biomass transfers (du Pontavice et al., 2019; Eddy et al., 2021; Maureaud et al., 2017). Differences in the rate of responses to climate change within marine communities and between regions disrupt existing ecosystem structure and functioning such as biomass flow in marine food webs (Barton et al., 2016; Dulvy et al., 2008; Kortsch et al., 2018; Montero-Serra et al., 2015; Verges et al., 2014).

Recent global projections based on several ecosystem models show that climate change is expected to induce a mean global biomass decrease in marine ecosystems (Lotze et al., 2019) mainly due to a decrease in production fueling marine food webs (NPP) amplified on animal biomass further up the food web by warming-induced changes in metabolic rates (Kwiatkowski et al., 2019; Lotze et al., 2019; Stock et al., 2014b, 2017). Different hypotheses are proposed to explain the climate-induced amplification of biomass decline including phyto- and zooplankton size composition, lengthening of food chains, reduced zooplankton growth efficiency and changes in metabolic rates (Kwiatkowski et al., 2019; Lotze et al., 2019; Stock et al., 2014b).

Only a few studies (e.g., Petrik et al., 2020) have explored both ecosystem biomass and production. For each ecosystem compartment, the latter is issued from animal growth and reproduction, implicitly referring to a gross production of living biomass (Gascuel et al., 2008, 2011; see Figure S1.1), which can be used in the system to feed the food web, detritus compartment, and fisheries if any, or to constitute a net production changing the current biomass of the considered compartment. The ecosystem production defines the capability of the ecosystem to replenish, e.g., following human impacts, and is therefore a key factor to study the future of fisheries whose sustainability is not directly related to biomass, but more to the exploited part of the gross production.

Analysis combining global fisheries catch data and information on fish life history traits showed that marine ecosystem trophodynamics, as indicated by the trophic transfer efficiency of energy through the food web and the residence time of biomass within each trophic level (TL), are sensitive to changes in ocean temperature (du Pontavice et al., 2019). However, the roles of these trophodynamic processes that govern the flow of energy through marine ecosystems in determining the relationship between NPP and upper TL production under climate change have not been explicitly explored.

Here, we aim to understand how future changes in ocean conditions would affect key ecosystem functions such as biomass transfers, consumer biomass and production (defined here for TLs ≥ 2), and ecosystem trophic structure. We use a trophodynamic ecosystem model – EcoTroph (Gascuel, 2005; Gascuel et al., 2011; Gascuel & Pauly, 2009) – to examine biomass flows within marine ecosystems and project future changes in biomass and production in the global ocean in the 21st century. The EcoTroph projections are forced with the outputs of three Earth system models (ESMs) under two emission scenarios (Representative Concentration Pathways, RCPs), RCP26 (strong mitigation scenario) and RCP8.5 ("no mitigation policy" scenario). Fishing exploitation and temporal dynamics were not explicitly considered in the model and, thus we projected climate change impacts on a theoretical unexploited ocean ecosystem under the steady state assumption. Based on the results from the simulation modeling, we examine the impacts of climate change on biomass flows and the resulting ecosystem biomass and production and discuss their implication for the sustainability of fisheries.

2. MATERIALS AND METHODS

2.1. The EcoTroph model

EcoTroph is an ecosystem modeling approach through which the ecosystem trophic functioning is modeled as a continuous flow of biomass surging up the food web, from lower to higher TLs, through predation and ontogenic processes (Figure 1, Gascuel et al., 2005, 2011). EcoTroph is founded on the principle that an ecosystem can be represented by a continuous distribution of the biomass along TLs, i.e., a biomass trophic spectrum (Gascuel et al., 2005). Biomass enters the food web at TL = 1, as generated by the photosynthetic activity of primary producers and recycling of nutrients by the microbial loop. Only mixotrophs, i.e., organisms that are simultaneously primary producers and first-order consumers, would be at TLs between TL = 1 and TL = 2. Their biomass is usually low, and is conventionally split between biomasses at TL = 1 and TL = 2. Biomass at TLs higher than 2 is composed of heterotrophic organisms with mixed diet and fractional TLs resulting in a continuous distribution of biomass along TLs (considered here as consumers).

To facilitate the computation of EcoTroph, biomass spectrum is aggregated by small TL classes that include all organisms within the lower and upper TLs of each class. Thus, EcoTroph does not represent individual species explicitly; instead, species are combined into classes based only on their TLs. As a convention (and based on previous studies; Gasche et al., 2012; Gascuel et al., 2005) we considered trophic classes of width $\Delta\tau = 0.1$ TL to be an appropriate resolution and a range starting at TL = 2 (corresponding to the first-order consumers), up to TL = 5.5, an appropriate range to cover all top predators in marine systems (Cortes, 1999; Pauly, 1998).

Another key principle behind EcoTroph is that trophic functioning of aquatic ecosystems may be viewed as a continuous biomass flow moving from lower to higher TLs. Each organic particle moves up the food web by continuous processes (representing an organism's ontogenetic changes

in TLs as it grows) and abrupt jumps due to predation events. By combining the flows of all particles in a food web, the aggregated biomass flows can be represented by a continuous function (see Figure S1.2). Thus, the continuous function of biomass flow in EcoTroph represents the mean flow of biomass of individual organisms and is not an approximation of a discrete process (Gascuel et al., 2008).

The flow of biomass in a biomass spectrum in EcoTroph is represented by the traditional equations of fluid dynamics. Specifically, the continuous biomass flow, $\Phi(t,\tau)$, is described by (details on equations and notations in Appendix S1):

$$\Phi(t, \tau) = B(t, \tau)K(t, \tau) \quad (1)$$

where $\Phi(t,\tau)$, the quantity of biomass moving up through TL τ, at every moment, t, due to predation, is expressed in t year^{-1}, $B(t,\tau)$ the density of biomass at TL = τ expressed in t TL^{-1}, and $K(t,\tau)$ the flow kinetic expressed in TL year^{-1}. The flow kinetic measures the speed of the biomass flow in the food web, from low to high TLs, and is inversely proportional to biomass residence time, i.e., the time each organism stays at a given level of the food web depending of its life expectancy.

Under steady-state conditions, the Equation 1 becomes:

$$B(\tau) = \frac{\Phi(\tau)}{K(\tau)} \quad (2)$$

The biomass flow $\Phi(\tau)$ is not conservative with a loss rate $\psi(\tau)$ at TL = τ, such as:

$$\frac{d\Phi(\tau)}{d\tau} = -\psi(\tau)\,\Phi(\tau) \quad (3)$$

Furthermore, the biomass flow $\Phi(\tau)$ can be expressed as a decreasing function of TL (see details in Appendix S1):

$$\Phi(\tau + \Delta\tau) = \Phi(\tau)e^{-\mu_\tau \Delta\tau} \quad (4)$$

Where $\Phi(\tau)$ is the biomass flow at TL τ (i.e., at the start of the trophic class $[\tau, \tau + \Delta\tau[$), μ_τ (expressed in TL^{-1}) represents the mean natural losses within the trophic class through non-predation mortality, excretion, and respiration. It defines the transfer efficiency, TE, within the trophic class $[\tau, \tau + \Delta\tau[$ such as:

$$TE = e^{-\mu_\tau} \quad (5)$$

A discrete approximation of the continuous distribution $B(\tau)$ is used for mathematical simplification (details on equations in Appendix S1). Hence, the model state variable becomes B_τ, the biomass (in metric tons) present at every moment under steady-state conditions within the TL class $[\tau, \tau + \Delta\tau[$ and Equation 2 becomes:

$$B_\tau = \frac{1}{K_\tau}\Phi_\tau \Delta\tau \quad (6)$$

where Φ_τ and K_τ are the mean biomass flow (in t $year^{-1}$) and the mean flow kinetic (in TL $year^{-1}$) within the trophic class $[\tau, \tau + \Delta\tau[$, respectively. The mean flow kinetic K_τ varies per trophic class and is directly defined using mean values per trophic class based on an empirical model previously developed by Gascuel et al. (2008) (see below).

Finally, EcoTroph defines the biomass flow $\Phi(\tau)$ as the density of production at TL = τ. Therefore, the production P_τ of the trophic class $[\tau, \tau+\Delta\tau[$ is:

$$P_\tau = \int_\tau^{\tau+\Delta\tau} \Phi(\tau)d\tau = \Phi_\tau \Delta\tau \quad (7)$$

Production is commonly expressed in t year^{-1} that implicitly refers to the conversion of biomass eaten at TL τ-1, into predator tissues whose mean TL is τ. Therefore, in a TL-based approach such as EcoTroph (wherein the width of trophic classes may different from 1 TL), production has to be expressed in t TL year^{-1}, i.e., tons moving up the food web by 1 TL on average during 1 year. Hence, EcoTroph highlights that biomass stems from the ratio of the production to the flow kinetic.

2.2. Simulating biomass flow from primary production to upper trophic levels

In EcoTroph, biomass flow and the resulting biomass from primary production to upper trophic levels are modeled using three distinct properties of marine food web potentially affected by climate change: (i) primary production fueling the food web (Eq. 7 at τ=1), (ii) trophic transfer efficiency quantifying biomass which is transferred at each trophic level (Eq. 5), and (iii) flow kinetic measuring the speed of this biomass transfer (Eq. 2 and 6).

2.2.1. Trophic transfer efficiency of low trophic levels

In this study, we modeled the trophodynamics of the planktonic food web separately from those of the upper part of the food web. Projections of annual average vertically integrated net primary production (NPP) from 1950 to 2100 were obtained from the outputs of global coupled atmosphere-ocean-biogeochemistry Earth system models (ESMs, described in the section below). EcoTroph considers NPP as biomass production at TL = 1 i.e., P_1 = NPP (Eq. 7). The flows of detritus biomass are not considered in this study and we discussed the implications of this assumption on the results and conclusions of this study.

While transfers of energy through the plankton food web can be complex (Friedland et al., 2012), a robust pattern revealed in numerous previous analyses is a tendency for more efficient energy transfers to fish in more productive regions (Armengol, Calbet, Franchy, Rodríguez-Santos, & Hernández-León, 2019; Ryther, 1969; Stock, Dunne, & John, 2014). This pattern arises because a)

the dominance of picophytoplankton in low productivity regions (Agawin et al., 2000; Armengol et al., 2019; Heneghan et al., 2016; Irwin et al., 2006; Morán et al., 2010) creates long food chains between primary producers and fish, and b) the limited surplus energy above basal metabolic costs of small zooplankton in subtropics reduces the planktonic transfer efficiency (Stock & Dunne, 2010; Stock, Dunne, & John, 2014).

To estimate variations in the plankton food web transfer efficiency across ocean biomes, we used simulations from the Carbon, Ocean Biogeochemistry, and Lower Trophics (COBALT) global ecosystem model, which has been shown to capture observed variations in the flow of energy across ocean biomes (Stock et al., 2014a, 2014b). Based on the outputs of COBALT, we estimated the transfer efficiency between the primary production and the mesozooplankton production, TE LTL, as:

$$\text{TE LTL}_{y,\,i} = \left(\frac{\text{MEZOO PROD}_{y,i}}{\text{NPP}_{y,i}}\right)^{1/(\text{MEZOO TL}_{y,i}\,-\,1)} \quad (8)$$

Where $NPP_{y,i}$ is the net primary production in the grid cell, i, for the year y, and MEZOO $PROD_{y,i}$ and MEZOO $TL_{y,i}$ are the mesozooplankton production and trophic level in the grid cell i for the year y. Transfer efficiency of low TLs (TE LTL) was calculated each year *y*, between 1950 and 2100 for RCP8.5 in every cell, i, of a two-dimensional horizontal 1°×1° grid covering the global ocean (Figure S2). $NPP_{y,i}$ and MEZOO $PROD_{y,i}$ were directly extracted from COBALT while MEZOO $TL_{y,i}$ was calculated using biomass flows between mesozooplankton and its preys in COBALT.

Transfer efficiency of low TLs is used to quantify the transfer efficiency between TL = 1 and TL = 2. Between TL = 2 and TL = 3, we assume a linear change from TE LTL (Eq. 8) at TL = 2 and TE HTL (described in the following section) at TL = 3. For TL > 3, we apply TE HTL to estimate

the transfer efficiency. The spatial pattern and the distribution of transfer efficiency of low TLs for each ecosystem over the reference period 1986–2005 are available in the Figures S3.3 and S3.4. To apply EcoTroph, the projected values of transfer efficiency at low TLs under the low and high greenhouse gas emissions scenarios are required. For the high greenhouse gas emissions scenario, we calculated the transfer efficiency of low TLs using the COBALT outputs projected for RCP8.5 as described above. For the low emissions scenario, since the COBALT model was not available for RCP2.6, we assumed that transfer efficiency follows the same global trend from 1950 to 2030 under RCP2.6 and RCP8.5. We made such assumption because the projected changes in SST, a key determinant of the transfer efficiency of low TLs, followed a similar pathway under RCP2.6 and RCP8.5 for this time period (see trends in SST and transfer efficiency of low TLs in the Figure S3.1). We defined the year 2031 as a breaking point from which the global trends in SST under RCP8.5 and RCP2.6 diverge (see Figure S3.2). Thus, for the time period from 2031 onwards, we assumed that the transfer efficiency of low TLs under RCP2.6 was the average of transfer efficiency of low TLs under RCP8.5 over the decade 2026–2036 (5 years before and after 2031) (detailed method in Appendix S3).

2.2.2. Trophic transfer efficiency of higher trophic levels

In EcoTroph, the trophic transfer efficiency of the higher TLs (TL >= 2) takes into account the losses at each trophic class and is used to estimate the fraction of biomass which is transferred from one TL to the next (Eq. 5). In this analysis, we use the temperature-dependent high TLs transfer efficiency (TE HTL) estimates derived from du Pontavice et al., (2019):

$$\mathrm{TE\ HTL} = e^{(-2.162 + \mathrm{SST}(-0.025 + a) + b)} \times 1.038 \quad (9)$$

where a and b are specific parameters for each ecosystem type (polar, temperate, tropical and upwelling; Table S4 and Figure S2) and SST is the sea surface temperature. This relationship

224 between SST and transfer efficiency of higher TLs was obtained by combining global fisheries
225 catch data and information on fish life history traits (du Pontavice et al., 2019). Thus, the warming-
226 induced variations in transfer efficiency of higher TLs reflect the changes in species assemblages
227 induced by ocean warming. These estimates of transfer efficiency of higher TLs were calculated
228 between TL = 2 and TL = 4 in all the coastal ecosystems and highlighted that biomass transfers are
229 characterized by "efficient-inefficient continuum" along a temperature gradient (see the
230 relationship between temperature and transfer efficiency of higher TLs in Figure S7f). Biomass
231 flows tend to be efficient in cold waters but less efficient in warmer waters. The temperature
232 dependent transfer efficiency of higher TLs estimates are negatively linked to SST with a strong
233 sensitivity to temperature in polar ecosystems and a lower sensitivity in tropical ecosystems
234 (du Pontavice et al., 2019). Besides, upwelling ecosystems stands out as an exception with low
235 transfer efficiency of higher TLs but a strong sensitivity to the changes in temperature (see the
236 warming effect on the transfer efficiency of higher TLs in Figure S7g)..

237 2.2.3. Flow kinetic

238 Flow kinetic measures the velocity of biomass transfers from lower to upper TLs and depends on
239 the biomass turnover. To estimate flow kinetic at TL = τ, we used an empirical equation (Gascuel
240 et al., 2008) as a function of SST and TL (τ):

$$K_\tau = 20.19\tau^{-3.26}e^{0.0.41SST} \quad (10)$$

241 The relationship between flow kinetic, and TL and SST derived from a statistical model based on
242 1,718 groups from 55 published Ecopath models (Gascuel et al., 2008). This study showed that P/B
243 can be considered as a measure of the trophic flow kinetic since P/B is a rate of regeneration of the
244 biomass over a unit of time (see detail in Gascuel et al., 2008). In contrast to the empirical equation
245 used for the transfer efficiency of higher TLs which is fitted for marine consumers (TLs >= 2; du

246 Pontavice et al., 2020), the flow kinetic equation was fitted through all marine groups from primary
247 producers to top predators (Gascuel et al., 2008) and includes the changes in kinetic along the food
248 web. Thus, flow kinetic depends on the position in the food web. While, at low TLs, biomass
249 transfers are faster due to species assemblages dominated by short-living species, biomass transfers
250 are slower at upper TLs mainly composed of long-living species (Gascuel et al., 2008).
251 Furthermore, the flow kinetic is negatively linked to SST since the species assemblages in warm
252 waters are characterized by shorter life expectancy than in colder waters (see the temperature effect
253 on flow kinetic in Figure S7c, d; Gascuel et al., 2008).
254
255 Hence, consumer production is determined by NPP, mainly driven by nutrient availability, light
256 limitation and temperature (Steinacher et al., 2010), and by the trophic transfer efficiencies, here
257 defined for low or high TLs, respectively, as emergent properties of food web dynamics and species
258 assemblages across the food web. Then, at each TL, consumer biomass is calculated as the product
259 of consumer production and the inverse of the flow kinetic. In this implementation of EcoTroph,
260 all climate effects are bottom-up and potential top-down effects are not included. The implications
261 on our projections will be further discussed. Figure 1 illustrates a conceptual schema of our
262 approach with the four variables at play to estimate ecosystem biomass and production. Each of
263 them, detailed above, is affected by climate change.

264 ## 2.3. EcoTroph simulations

265 EcoTroph model is applied separately to 41,135 grid cells in a two-dimensional horizontal 1°
266 latitude x 1° longitude grid covering the global ocean (Figure S2). Biogeography of grid cells were
267 delimited using the distribution of biomes identified by Reygondeau et al., (2013) and adapted from
268 Longhurst (2007). Each cell was classified as one of the 3 biomes: tropical, temperate and polar

biomes. Polar biome was divided into the Arctic and Antarctic ecosystem types to consider the specificity of each of the areas, especially in terms of projected changes in primary production. Upwelling ecosystems were added using the biogeographical provinces described by Reygondeau et al., (2013) (Figure S2). Biomass and production were calculated for TLs between 2 and 5.5 at intervals of $\Delta\tau = 0.1$, for every year between 1950 and 2100, using projected NPP and SST in each grid cell as inputs. The data comes from three Earth system models (ESMs) developed by three institutes: Geophysical Fluid Dynamics Laboratory (GFDL-ESM2M; Dunne et al., 2012), Max Plank Institute (MPI-ESM-MR; Giorgetta et al., 2013) and Institut Pierre Simon Laplace (IPSL-CM5A-MR; Dufresne et al., 2013). Moreover, we considered two contrasting scenarios: RCP2.6, radiative forcing level reaches 3.1 W m^{-2} by mid-century, and returns to 2.6 W m^{-2} by 2100 (strong mitigation scenario) and RCP8.5, rising radiative forcing pathway leading to 8.5 W m^{-2} in 2100 ("no mitigation policy" scenario). All the changes in parameters, production and biomass were calculated relatively to the IPCC's AR5 (in which the three above described ESMs were used; IPCC, 2014) reference period 1986-2005.

To quantify the uncertainty induced by the three ESMs, the inter-model variability was estimated by calculating the standard deviation of the changes coming from the three ESMs in 2090–2099 relative to 1986–2005. Then, we mapped the grid cells where the three models do not predict the same direction of the changes (e.g., one predicts an increase while the two others predict a decrease) (see Figures S5a and S5b).

A set of additional simulations was designed to estimate the contribution of each process determining the biomass flow on the total consumer biomass and trophic structure. We examined the response of consumer biomass to the four following biomass flow processes: (1) NPP, (2) transfer efficiency of higher TLs, (3) transfer efficiency of low TLs and (4) flow kinetic. In order to understand how biomass of marine ecosystems responds to changes in ocean conditions, we

293 isolated successively the response of each of the four processes. For this analysis, we ran four sets
294 of simulations for each of the three ESMs using RCP8.5. Each of the simulations isolates one
295 biomass flow parameter, which varies over the period 1950–2100 while the others remain constant
296 and equal to their mean values during the reference period 1986–2005. For example, to isolate the
297 effects of NPP, we set kinetic, transfer efficiencies of higher TLs and low TLs at their mean values
298 during the reference period, while NPP vary over 1950–2100.

3. RESULTS

3.1. Changes in ocean conditions and biomass transfers over the 21st century

This study projects that the flows of biomass in marine ecosystems will change substantially by 2100 under scenarios of climate change. First, the global NPP exhibits a mean projected decrease of 7.2% and 1.0% for RCP8.5 and RCP2.6, respectively, in 2090–2099 relative to 1986–2005 with large differences among ESMs under RCP8.5 (Figure 2a). Specifically, at global scale and under RCP8.5, NPP is projected to decrease by 13.4% and 8.1% for MPI and IPSL, respectively, but no change in NPP is projected by GFDL in 2090–2099 relative to 1986–2005. Large decreases in NPP are projected in low-latitude tropical ecosystems (12.3% by 2090–2099 relative to 1986–2005), largely driven by warming-induced stratification (Cabré et al., 2015; Laufkötter et al., 2015) (Figure 2b). In contrast, in high-latitude polar ecosystems, NPP is projected to increase with large variations between ESMs (Figure 2c).

The global average low TL transfer efficiency is projected to decline by 3.5% and 1.0% under RCP8.5 and RCP2.6, respectively (Figure 2d). While the projected changes in transfer efficiency are small in Antarctic, temperate and upwelling ecosystems, the transfer efficiency is projected to decrease largely in tropical ecosystems (-8.8%) and increase in Arctic ecosystems (Figure 2e).

The changes in transfer efficiency of higher TLs are projected to decrease, on average, by 4.6% and 1.1% under RCP8.5 and RCP2.6, respectively by the end of the 21st century relative to 1986–2005 (Figure 2g). However, since the sensitivity of temperature varies among ecosystem types (du Pontavice et al., 2019) and the sea surface warming is projected to vary spatially (Appendix S7b), the higher TLs transfer efficiency is projected to decrease substantially in upwelling and temperate ecosystems (-14.7% and -8.5%, respectively, in 2090–2099 relative to

1986–2005) while in the other ecosystem types, the mean projected decline is relatively low (Figure 2h).

Finally, the mean flow kinetic within marine food web (between TL = 2 and TL = 5.5) is projected to increase, on average, by 11.8% and 2.6% for RCP8.5 and RCP2.6, respectively by 2090–2099 relative to 1986–2005 (Figure 2j). The changes in mean flow kinetic follow closely the changes in sea surface temperature. The projected ocean warming thus result in increases in flow kinetic in almost all ecosystems except in Antarctic ecosystem (Figure 2k) where the projected changes in SST by 2100 is small (Figure S7b).

3.2. Global decline of total consumer biomass

The model projects a global mean decrease in total consumer biomass (i.e., total animal biomass with TLs>=2) in the ocean by 18.5% (from 12% with GFDL to 22.9% with IPSL) with RCP8.5 and 4.5% with RCP2.6 by 2090–2099 relative to 1986–2005 (Figure 3a).

We found that the projected increase in flow kinetic contributes the most to the global projected decrease in total consumer biomass relative to the contributions from changes in NPP and trophic efficiencies (Figure 3b). The intermodel variations in global biomass projections are largely a result of the differences in NPP projections between the three ESMs (Figure 3b).

Climate-induced changes in total consumer biomass are projected to vary widely between different parts of the global ocean (Figure 4a and b). Specifically, major gains in biomass are projected in the Arctic Ocean, along the coast of Antarctica and in the south-eastern Pacific Ocean. The ensemble mean total consumer biomass is projected to decline strongly between 40° S and 50° N latitude (Figure 4c). Notably, under RCP8.5, total consumer biomass is projected to decrease in 2090–2099 relative to 1986–2005, on average, by 28%, 18%, 16% and 10% in tropical, upwelling, temperate and Arctic ecosystems, respectively (Figure 5a). Overall, the spatial patterns of changes

in total consumer biomass are similar between RCP8.5 and RCP2.6 but the magnitude of changes is larger under RCP8.5. The areas wherein the projected decrease in biomass exceeds 25% represent 43% of the total ocean surface area for RCP8.5 in 2090–2099 and only 2.5% for RCP2.6. In all the ecosystems, warming-induced increases in flow kinetic negatively affect total consumer biomass while the effects of climate change on transfer efficiencies and NPP vary between ecosystem types. In Arctic ecosystem, total consumer biomass is negatively affected by the increases in flow kinetic and transfer efficiency of higher TLs. Simultaneously, the projected decrease in transfer efficiency of low TLs positively affects total consumer biomass. In Antarctic ecosystems, the projected increase in NPP compensates the warming-induced increase in flow kinetic. In temperate ecosystems, flow kinetics and transfer efficiencies (at low and higher TLs) are projected to be the main drivers of the changes in total consumer biomass, while in upwelling ecosystem the decrease in biomass is mainly driven by the decrease in flow kinetics, NPP and transfer efficiency of higher TLs. In tropical ecosystems, the sharp projected decline in total consumer biomass is explained by the climate-induced changes in flow kinetics, NPP and transfer efficiency of low TLs.

3.3. Changes in trophic structure of marine ecosystems

Our results also highlight the effects of climate change on biomass at each TL from primary consumers to the top predators since the EcoTroph model represents the food web as a biomass distribution per TL (Figure 6). We show that the projected distribution of biomass across different TLs for RCP2.6 remains close to those of the contemporary ocean (1986–2005, Figure 6a and Figure 7a) while the distribution of the biomass for RCP8.5 is modified, with the largest impacts on high TL species (Figures 6b and 7b). For RCP8.5, the model projects, on average, a 21.3% decline in predator biomass in 2090–2099 relative to 1986–2005 for TLs between 3.5 and 5.5 which

mainly refer to predatory fishes (e.g., cods, tunas, groupers). In contrast an 18.8% decrease in biomass is projected for TLs between 2.5 and 3.5 which usually refers to forage fishes (e.g., herring, capelin) and invertebrates (e.g., shrimps, crabs). Under the strong mitigation scenarios (RCP2.6), the declines in biomass at higher TLs are less pronounced (Figure 6b and black line in Figure 7b). Faster biomass flow (i.e., larger flow kinetic) projected under climate change produces a nearly uniform ~10% reduction in biomass across TLs by the end of the 21st century relative to 1986-2005 (Figure 6c). However, the decrease in transfer efficiency at higher TLs causes a more pronounced decline in biomass at higher TLs. Since the higher TLs represent only a small fraction of total biomass, the changes in biomass at higher TLs have relatively small effect on total consumer biomass (Figure. 6a). However, species at higher TLs include some of the most valuable species, thus the impacts for global fisheries may be exacerbated where the transfer efficiency at higher TLs is the most affected by ocean warming.

The changes in trophic structure differ from one ecosystem type to the other, for both RCPs (Figure 7a and b). The differences in biomass decline between low and high TLs are particularly important in upwelling, temperate and Arctic ecosystems (Figure 7a and b) where the warming-induced changes in transfer efficiency of higher TLs are the highest (see Figure 2h).

3.4. Changes in ecosystem production

While our projections indicate a decline in total consumer biomass by, on average, 18.4%, total consumer production is projected to decrease by 12.0% “only”, by 2090–2099 relative to 1986–2005 under RCP8.5 (Figure 8a). The lower decrease in production is mechanistically due to the warming-induced increase in flow kinetic (+11.8% under RCP8.5) since production is the product of biomass and flow kinetic. Hence, we projected that total consumer production may increase in the Arctic and Antarctic ecosystems by, on average, 1.7% and 1.8%, respectively, by 2090–2099

despite the great inter-ESM uncertainty (blue bars in Figure 8b). In the other ecosystem types (Figure 8b), the declines in total consumer production are projected to be attenuated compared to those in biomass with differences in change of about 10% (e.g., in tropical ecosystem, the projected decrease in the ensemble mean total consumer biomass reaches 28.3% while total consumer production is projected to decrease by 18.4%). Similar to the trend in biomass, production of higher TLs is projected to be more affected than lower TLs (Figure 8c). Specifically, EcoTroph projects, on average, a 16.3% decline in predator production (TLs between 3.5 and 5.5) while prey production (TLs between 2.5 and 3.5) is projected to decrease by 13.1% (Figure 8c).

4. DISCUSSION

Through modeling marine ecosystems as trophic spectrum, we project a drastic decline in consumer biomass and production throughout the 21st century under the "no mitigation policy" scenario (RCP 8.5) driven by a change in the biomass flow in marine food webs. The projected changes in biomass also vary widely spatially because of regional differences in changes in ocean biogeochemical and physical conditions and the characteristics of the ecosystems. In addition, we found an amplification of climate-induced changes in biomass and production at higher TLs relative to lower TLs in various ecosystems (temperate, upwelling and Arctic), potentially leading to pronounced declines of highly commercially valuable large fish species.

4.1. Drivers of changes in consumer biomass

This study shows that changes in net primary production, flow kinetics and transfer efficiencies drive changes in global ocean biomass and production. Specifically, we highlighted that the changes in total consumer biomass and production are largely driven by the balance between the effects of trophodynamic constraints (imposed by net primary production) and the temperature-dependent flow kinetic and transfer efficiencies (at higher TLs). At global scale, the main driver of the changes of total consumer biomass is the flow kinetic which is directly affected by global ocean warming. In other words, in a warming ocean which favors short-living species, each unit of biomass spends less time at a given TL and subsequently at all TLs, which leads the total biomass to decrease (Gascuel et al., 2008). In parallel, the warming-induced decrease in transfer efficiency of higher TLs affects both consumer production and biomass due to larger energy losses between each TL (du Pontavice et al., 2019). The increase in sea water temperature affects both the quantify of matter and energy which is transferred through the food (decrease in trophic transfer efficiency) and the speed at which biomass transfer occurs (increase in flow kinetic). Thus, temperature-

induced changes in flow kinetic and trophic transfer efficiency may contribute independently and cumulatively to the decline in consumer biomass.

Previous studies suggest that changes in these trophodynamic processes are caused by changes in species assemblages induced by the increase in sea water temperature (du Pontavice et al., 2019; Gascuel et al., 2008; Maureaud et al., 2017). Hence biomass transfers tend to be faster but less efficient at each TL in warmer waters (du Pontavice et al., 2019; Gascuel et al., 2008) due to species assemblages more and more dominated by fast-growing, short-living, early-maturing species as suggested by Beukhof et al. (2019).

4.2. Trophic amplification induced by less efficient transfer

Our findings suggest an amplification of the changes in biomass from low to high TL components of the ecosystem, with a more pronounced decrease in high TLs. This process describes the propagation of the climate signal from low to upper TLs through the decline (or increase) of biomass along the food web. Trophic amplification has been previously shown for phytoplankton and zooplankton using different planktonic food web models and different Earth system models (Chust et al., 2014; Kwiatkowski et al., 2019; Stock et al., 2014b). At the upper trophic levels, Petrik et al. (2020), based on a spatially explicit mechanistic model of three functional types of fish, showed the amplification of the projected changes in productivity by grouping functional types by trophic level. In a complementary way and using a trophic-level-based model, our projections highlighted a continuous and progressive amplification of changes in biomass and production when moving up the food web. This process arises from the cumulative effect all along the food web of the warming-induced decline in transfer efficiency at each trophic level. The alteration of the trophic structure of marine ecosystems supports the concerns regarding the consequences of trophic downgrading (Estes et al., 2011) which can be characterized by trophic

444 cascades due to the decrease in predator biomass. Indeed, several studies showed the impacts of
445 top predators depletion on marine ecosystem functioning (Baum & Worm, 2009; Estes et al., 2016;
446 Ferretti et al., 2010; Heithaus et al., 2008) and stability (Britten et al., 2014; Rasher et al., 2020).
447 Despite their low biomass (compared to the lower TLs), predators at TL higher than 3.5 currently
448 support more than 35% of the world fisheries (Branch et al., 2010). Therefore, our results suggest
449 that changes in transfer efficiencies induced by climate change may be a key player in the expected
450 decrease of the word potential fisheries catch (Bindoff et al., 2019; FAO, 2018).
451 In a recent compilation of marine ecosystems models (the FISH-MIP model intercomparison
452 project; Lotze et al., 2019), a trophic amplification process was highlighted with combined biomass
453 of higher trophic levels declining more strongly than lower trophic levels. While this amplification
454 was consistent across the majority of FISH-MIP models, differences in fundamental structures and
455 ecological processes lead to large differences in the projected shifts in total consumer biomass,
456 with global declines by 2100 ranging from ~12% to ~20% in RCP8.5. The trophodynamic
457 constraints due to changes in ocean conditions filtered through EcoTroph support the high end of
458 this response (Appendix S6).

459 ### 4.3. Toward a global decline in fisheries catch?

460 While FISH-MIP results focused on biomass (Lotze et al., 2019), our results also highlighted the
461 significant impact of climate change on the gross natural production of marine ecosystems. This
462 result is a key issue for fisheries whose sustainability is not directly related to biomass, but more
463 to production and to the exploited part of production. The EcoTroph approach reveals that
464 production may be impacted by lower NPP, and less efficient trophic transfers along the food web.
465 However, the expected faster energy flow may not have any effect on production, but a large impact
466 on the biomass. In other words, using projections changes in biomass to infer the coming effect of

climate change on catch potential may lead to an overestimation of this effect. The loss in biomass will be partially counterbalanced by faster turnover which makes each unit of biomass more productive. Considering predator at TLs higher than 3.5, the projected change in potential catch (by 2100 under RCP8.5) would be closer to 16.3%, based on production, than to 21.3% as expected from biomass. Trophic amplification in production (and not in biomass) is consistent with the projections based on a mechanistic model resolving trophic interactions and basic life cycle processes (Petrik et al., 2020). Interestingly, while we projected a decrease of 12.0% in total fish production, Petrik et al. (2020) projected total fisheries yield declines by 11.8% using a simple representation of fishing (constant over space, time and TL). However, they projected larger differences in fisheries yield between the low and the high TLs.

Our projections imply potential repercussions on the global catch potential and on its distribution, with different consequences in the different ecosystem types. Tropical ecosystems would be the most impacted (-28.3% and -18.4% in biomass and production, respectively) but with a low amplification due to low changes in transfer efficiency. Thus, large decreases in fisheries yield would be experienced at all TLs from forage fish to predator species in these regions where many nations show a high socioeconomically dependency on fisheries (Bindoff et al., 2019; Golden et al., 2016). Conversely, in temperate and polar ecosystems, the decline in fisheries yield may be lower especially if we consider the projected decline in production (instead of biomass). However, in these ecosystems we projected large changes in food web structure (through trophic amplification processes) which may result in major changes in catch structure. While fisheries targeting low and mid TLs species may be moderately affected by climate change, fisheries targeting upper TLs species may be much more impacted. To mitigate socioeconomically impacts of these changes, fisheries management should adapt its methods to address declines in total catch but also changes in catch structure.

4.4. Modelling considerations and sources of uncertainties

Our modelling approach is the first application of EcoTroph linking the trophic ecology and the projected changes in ocean conditions. Within the TL-based models (e.g., Ecopath with Ecosim), EcoTroph may be viewed as a synthetic approach in the use of the TL concept for ecosystem modelling in which individual species are combined into classes. Therefore, EcoTroph does not explicitly resolve the climate-induced impacts on individual species and population. Instead, the model assumes that the shifts in environmental conditions will lead to the emergence of new biomass transfer features in theoretical steady state ecosystems.

So far, in our implementation of EcoTroph, the model accounts for steady states (see equations 2 and 4). Hence, one of the challenges in future studies will be to develop a new generation of the model, integrating time dynamic processes in order to analyze the propagation of impacts and their aggregation on a larger scale. Such a dynamic EcoTroph model may, for instance, allow at exploring the expected effects of widespread increases in marine heat waves frequency and intensity which is a major source of concern for the future productivity and stability of marine ecosystems. A recent modeling work focusing on the northeast Pacific has showed that by 2050 marine heat waves could more than double the magnitude of the impacts on fish stocks biomass and spatial distribution due to long-term climate change (Cheung & Frölicher, 2020).

Although EcoTroph can include top-down effects induced by fishing pressure (e.g., Gasche et al., 2012; Halouani et al., 2015), in the present implementation of the model the effects of trophic cascades are not included, thus the model is only driven by bottom-up processes. Since we projected that the largest species are the ones most affected, the release of top-down predation pressure may induce an increase in production of the smaller prey species. Hence, the introduction of top-down effects should exacerbate the projected changes in trophic structure.

514 The major source of uncertainty in our projections of production and biomass is due to a large inter-
515 model variability in NPP projections (Appendix S5; Bopp et al., 2013; Laufkötter et al., 2015). As
516 in EcoTroph, ocean primary production (or the related phytoplankton biomass) is a pivotal
517 component of several marine ecosystem models by sustaining and limiting the biomass of higher
518 TLs (e.g., Blanchard et al., 2012; Carozza et al., 2016; Cheung et al., 2011; Jennings &
519 Collingridge, 2015). Hence, identifying the sources of the current uncertainty associated with
520 future NPP and constraining estimates is one of the major challenges in understanding the
521 responses of marine food web to climate change (Kwiatkowski et al., 2017; Vancoppenolle et al.,
522 2013). These variations in NPP projections are particularly large in Arctic ecosystems with
523 substantial differences in the direction of changes among the ESMs (see Appendix S5). In contrast
524 to NPP, the projections in flow kinetic and transfer efficiency of the higher TLs, which are
525 functions of temperature, appear relatively consistent across the three ESMs.
526 In our study, we considered variations in planktonic food web structure through the estimates of
527 transfer efficiency of low TLs. Accounting for these variations is essential to understand biomass
528 and production dynamics in marine ecosystems, since transfer efficiency of low TLs constraints
529 the fraction of energy available for the upper TLs (Friedland et al., 2012; Petrik et al., 2019). The
530 introduction of transfer efficiency of low TLs is expected to provide more realistic estimates of
531 climate change effects, though we recognize that it does not capture the full diversity of pathways
532 connecting phytoplankton and fish. While this study considered variations in the pelagic plankton
533 food web transfer efficiency across trophic gradients, future efforts could consider more complete
534 pelagic, benthic and mesopelagic pathways (Friedland et al., 2012; Petrik et al., 2019; Stock et al.,
535 2017).
536 Moreover, the flows of detritus biomass are not considered in this study. In open ocean, the bulk
537 of the transfer of energy occurs between phytoplankton and zooplankton but, in continental shelf

538 ecosystems, NPP also fuels benthic pathway through downward coupling (Cresson et al., 2020;
539 Duffill Telsnig et al., 2018; Woodland & Secor, 2013). Hence, by considering only the pelagic
540 energy transfer in plankton food web, we have likely underestimated the fraction of energy which
541 fuel the food web.
542 The projected changes in transfer efficiency of higher TLs and flow kinetic can be a result of
543 changes in species assemblages under ocean warming (du Pontavice et al., 2019; Gascuel et al.,
544 2008), but other negative climate-induced biological responses at individual (e.g., decrease in body
545 size; Cheung et al., 2012) and population levels (e.g., change in phenology; Thackeray et al., 2016)
546 that may amplify the overall climate change impacts on flow kinetic and trophic transfer efficiency,
547 are not represented. Thus, our approach can be considered conservative and the decline in the global
548 marine biomass and production we projected is likely to be underestimated.
549
550 Overall, our modelling approach signal the significant impact of climate change on marine animal
551 biomass but also on production over the 21st century. The latter, which is a key issue for fisheries,
552 is projected to decline but to a lesser extent than biomass due to a compensation effect induced by
553 faster trophic transfer under ocean warming. Hence, we emphasize the importance of considering
554 production to provide insights regarding the future catch potential. Furthermore, the projected
555 changes in trophic structure through a trophic amplification process show that marine predator
556 (TL>=3.5) may be particularly affected by climate change.

ACKNOWLEDGMENT

We wish to thank the Nippon Foundation-UBC Nereus program for supporting the collaboration between L'Institut Agro, Rennes, and the University of British Columbia, Vancouver. Hubert du Pontavice, William W.L. Cheung and Gabriel Reygondeau acknowledge funding support from the Nippon Foundation-UBC Nereus Program. William W. L. Cheung also acknowledges funding support from the Natural Sciences and Engineering Research Council and Social Sciences and Humanities Research Council of Canada. We further thank Jerome Guitton for his technical support.

LIST OF LEGENDS

FIGURE 1: Conceptual design of the EcoTroph model and forcing used. The trophic functioning of marine food webs is represented by a biomass flow, with biomass entering the system at trophic level 1 due to net primary production, NPP. Biomass flow reaching each trophic level is then defined by the trophic transfer efficiency at low and high trophic level, TE LTL (derived from the plankton food web model COBALT) and TE HTL (estimated from the sea surface temperature (SST) according to du Pontavice et al. (2019)), respectively. The flow kinetics, which is also forced by SST (Gascuel et al., 2008), is a key parameter to derive biomass at each trophic level of the model from the biomass flow (Gascuel & Pauly, 2009). One EcoTroph model is implemented each year within each cell of the global ocean, forced by NPP and SST from Earth system models' projections.

FIGURE 2: Projected changes in biomass flow processes between 1950 and 2100 relative to 1986–2005. The changes in net primary production, NPP, (a, b, c), transfer efficiency of low trophic levels, TE LTL, (d, e, f), transfer efficiency of higher trophic levels, TE HTL, (g, h, i) and flow kinetic (j, k, l) are represented on this figure. Panels (a), (d), (g) and (j) represent the changes at global scale for RCP2.6 and RCP8.5. Panels (b), (e), (h) and (k) represent the changes in each ecosystem type under RCP8.5. The shaded areas around the curves in these panels indicate the inter-model variability (i.e., the variability given by the inputs of the 3 different Earth system models) and the color bars outside the box indicate the range of averaged changes of the three Earth system models over 2090–2099. Panels (c), (f), (i) and (l) represent the changes over the period 2090–2099 in each 1°x1° grid cell.

FIGURE 3: Changes in total consumer biomass over the period 1950–2100. (a) Changes in total consumer biomass for RCP2.6 and RCP8.5 relative to the reference period 1986–2005. (b) Mean changes in total consumer biomass for RCP8.5 relative to 1986–2005 in which the contribution of net primary production (NPP), transfer efficiency of lower trophic level (TE LTL), transfer efficiency of higher trophic level (TE HTL) and flow kinetic are isolated. The shaded areas around the curves indicate the inter-model variability and the color bars indicate the ranges of averaged changes of three Earth system models over 2090–2099.

FIGURE 4: Maps of the ensemble mean projections for the three Earth system models of changes in total consumer biomass by 2090–2099 relative to 1986–2005 under (a) RCP2.6 and (b) RCP8.5. Panel (c) represents the changes in consumer biomass by latitude for RCP2.6 and RCP8.5.

FIGURE 5: Changes in total consumer biomass in each ecosystem type as well as the processes at play for RCP8.5. Panel (a) represents the changes in total consumer biomass for RCP8.5 in each ecosystem type relative to the reference period 1986–2005. Panel (b) represents the mean contribution of the four processes in each ecosystem type (net primary production (NPP), transfer efficiency of lower trophic level (TE LTL), transfer efficiency of higher trophic level (TE HTL) and flow kinetic). The contribution is framed in red color if biomass projections with one of the three models predicts changes in the opposite direction to those predict with the two other models.

FIGURE 6: Changes in trophic structure under RCP2.6 and 8.5. (a) Biomass trophic spectra for RCP2.6 and RCP8.5 in 2090–2099 and the reference period in 1986–2005, while (b) Changes in biomass for each trophic class of width 0.1 trophic level (TL) between TL = 2 and TL = 5.5 under RCP2.6 and RCP8.5 relative to the reference period 1986–2005. (c) The ratio of biomass trophic spectra in 2090–2099 for RCP8.5 and for the reference period 1986–2005 derived from EcoTroph projections in which each flow parameter is successively isolated (net primary production (NPP), transfer efficiency of lower trophic level (TE LTL), transfer efficiency of higher trophic level (TE HTL) and flow kinetic)**.**

FIGURE 7: Changes in trophic structure in each ecosystem type for RCP2.6 and 8.5. The two panels show the ratio of the biomass spectrum in 2090-2090 to the reference period 1986–2005 for RCP2.6 (a) and RCP8.5 (b) for each ecosystem type.

FIGURE 8: Changes in production at global scale and in each ecosystem type over the 21st century. Panel (a) represents the changes in total consumer production and biomass and in kinetic under RCP8.5 by 2100 relative to the reference period 1986–2005 while panel (b) represents the changes in total consumer production for RCP8.5 in each ecosystem type. Panel (c) represents the changes in prey (between trophic level (TL) = 2.5 and TL = 3.5) and predator (up to TL = 3.5) under RCP2.6 and RCP8.5.

REFERENCES

Agawin, N. S. R., Duarte, C. M., & Agustí, S. (2000). Nutrient and temperature control of the contribution of picoplankton to phytoplankton biomass and production. *Limnology and Oceanography*, *45*(3), 591-600. https://doi.org/10.4319/lo.2000.45.3.0591

Armengol, L., Calbet, A., Franchy, G., Rodríguez-Santos, A., & Hernández-León, S. (2019). Planktonic food web structure and trophic transfer efficiency along a productivity gradient in the tropical and subtropical Atlantic Ocean. *Scientific Reports*, *9*(1), 2044. https://doi.org/10.1038/s41598-019-38507-9

Asch, R. G., Stock, C. A., & Sarmiento, J. L. (2019). Climate change impacts on mismatches between phytoplankton blooms and fish spawning phenology. *Global Change Biology*, gcb.14650. https://doi.org/10.1111/gcb.14650

Barton, A. D., Irwin, A. J., Finkel, Z. V., & Stock, C. A. (2016). Anthropogenic climate change drives shift and shuffle in North Atlantic phytoplankton communities. *Proceedings of the National Academy of Sciences*, *113*(11), 2964-2969. https://doi.org/10.1073/pnas.1519080113

Baum, J. K., & Worm, B. (2009). Cascading top-down effects of changing oceanic predator abundances. *Journal of Animal Ecology*, *78*(4), 699-714. https://doi.org/10.1111/j.1365-2656.2009.01531.x

Beukhof, E., Frelat, R., Pecuchet, L., Maureaud, A., Dencker, T. S., Sólmundsson, J., Punzón, A., Primicerio, R., Hidalgo, M., Möllmann, C., & Lindegren, M. (2019). Marine fish traits follow fast-slow continuum across oceans. *Scientific Reports*, *9*(1), 17878. https://doi.org/10.1038/s41598-019-53998-2

Bindoff, N. L., Cheung, W. W. L., Kairo, J. G., Guinder, V. A., Hallberg, R., Hilmi, N., Jiao, N., Karim, M. S., Levin, L., O'Donoghue, S., Purca Cuicapusa, S. A., Rinkevich, B., Suga, T., Tagliabue, A., & Williamson, P. (2019). Changing Ocean, Marine Ecosystems, and Dependent Communities. In *IPCC Special Report on the Ocean and Cryosphere in a Changing Climate*.

652 Blanchard, J. L., Jennings, S., Holmes, R., Harle, J., Merino, G., Allen, J. I., Holt, J., Dulvy, N. K., & Barange,
653 M. (2012). Potential consequences of climate change for primary production and fish production
654 in large marine ecosystems. *Philosophical Transactions of the Royal Society B: Biological Sciences*,
655 *367*(1605), 2979‐2989. https://doi.org/10.1098/rstb.2012.0231
656 Bopp, L., Resplandy, L., Orr, J. C., Doney, S. C., Dunne, J. P., Gehlen, M., Halloran, P., Heinze, C., Ilyina, T.,
657 Séférian, R., Tjiputra, J., & Vichi, M. (2013). *Multiple stressors of ocean ecosystems in the 21st*
658 *century : Projections with CMIP5 models*. 21.
659 Branch, T. A., Watson, R., Fulton, E. A., Jennings, S., McGilliard, C. R., Pablico, G. T., Ricard, D., & Tracey, S.
660 R. (2010). The trophic fingerprint of marine fisheries. *Nature*, *468*(7322), 431‐435.
661 https://doi.org/10.1038/nature09528
662 Britten, G. L., Dowd, M., Minto, C., Ferretti, F., Boero, F., & Lotze, H. K. (2014). Predator decline leads to
663 decreased stability in a coastal fish community. *Ecology Letters*, *17*(12), 1518‐1525.
664 https://doi.org/10.1111/ele.12354
665 Burrows, M. T., Schoeman, D. S., Richardson, A. J., Molinos, J. G., Hoffmann, A., Buckley, L. B., Moore, P.
666 J., Brown, C. J., Bruno, J. F., Duarte, C. M., Halpern, B. S., Hoegh-Guldberg, O., Kappel, C. V.,
667 Kiessling, W., O'Connor, M. I., Pandolfi, J. M., Parmesan, C., Sydeman, W. J., Ferrier, S., …
668 Poloczanska, E. S. (2014). Geographical limits to species-range shifts are suggested by climate
669 velocity. *Nature*, *507*(7493), 492‐495. https://doi.org/10.1038/nature12976
670 Cabré, A., Marinov, I., & Leung, S. (2015). Consistent global responses of marine ecosystems to future
671 climate change across the IPCC AR5 earth system models. *Climate Dynamics*, *45*(5‐6), 1253‐1280.
672 https://doi.org/10.1007/s00382-014-2374-3
673 Carozza, D. A., Bianchi, D., & Galbraith, E. D. (2016). The ecological module of BOATS-1.0 : A
674 bioenergetically constrained model of marine upper trophic levels suitable for studies of fisheries

and ocean biogeochemistry. *Geoscientific Model Development*, *9*(4), 1545‐1565. https://doi.org/10.5194/gmd-9-1545-2016

Cheung, W. W. L., Dunne, J., Sarmiento, J. L., & Pauly, D. (2011). Integrating ecophysiology and plankton dynamics into projected maximum fisheries catch potential under climate change in the Northeast Atlantic. *ICES Journal of Marine Science*, *68*(6), 1008‐1018. https://doi.org/10.1093/icesjms/fsr012

Cheung, W. W. L., & Frölicher, T. L. (2020). Marine heatwaves exacerbate climate change impacts for fisheries in the northeast Pacific. *Scientific Reports*, *10*(1), 6678. https://doi.org/10.1038/s41598-020-63650-z

Cheung, W. W. L., Sarmiento, J. L., Dunne, J., Frölicher, T. L., Lam, V. W. Y., Deng Palomares, M. L., Watson, R., & Pauly, D. (2012). Shrinking of fishes exacerbates impacts of global ocean changes on marine ecosystems. *Nature Climate Change*, *3*(3), 254‐258. https://doi.org/10.1038/nclimate1691

Chust, G., Allen, J. I., Bopp, L., Schrum, C., Holt, J., Tsiaras, K., Zavatarelli, M., Chifflet, M., Cannaby, H., Dadou, I., Daewel, U., Wakelin, S. L., Machu, E., Pushpadas, D., Butenschon, M., Artioli, Y., Petihakis, G., Smith, C., Garçon, V., … Irigoien, X. (2014). Biomass changes and trophic amplification of plankton in a warmer ocean. *Global Change Biology*, *20*(7), 2124‐2139. https://doi.org/10.1111/gcb.12562

Cortes, E. (1999). Standardized diet compositions and trophic levels of sharks. *ICES Journal of Marine Science*, *56*(5), 707‐717. https://doi.org/10.1006/jmsc.1999.0489

Cresson, P., Chouvelon, T., Bustamante, P., Bănaru, D., Baudrier, J., Le Loc'h, F., Mauffret, A., Mialet, B., Spitz, J., Wessel, N., Briand, M. J., Denamiel, M., Doray, M., Guillou, G., Jadaud, A., Lazard, C., Noûs, C., Prieur, S., Rouquette, M., … Harmelin-Vivien, M. (2020). Primary production and depth drive different trophic structure and functioning of fish assemblages in French marine ecosystems. *Progress in Oceanography*, 102343. https://doi.org/10.1016/j.pocean.2020.102343

698 Duffill Telsnig, J. I., Jennings, S., Mill, A. C., Walker, N. D., Parnell, A. C., & Polunin, N. V. C. (2018). Estimating
699 contributions of pelagic and benthic pathways to consumer production in coupled marine food
700 webs. *Journal of Animal Ecology*, 1365-2656.12929. https://doi.org/10.1111/1365-2656.12929
701 Dufresne, J.-L., Foujols, M.-A., Denvil, S., Caubel, A., Marti, O., Aumont, O., Balkanski, Y., Bekki, S.,
702 Bellenger, H., Benshila, R., Bony, S., Bopp, L., Braconnot, P., Brockmann, P., Cadule, P., Cheruy, F.,
703 Codron, F., Cozic, A., Cugnet, D., … Vuichard, N. (2013). Climate change projections using the IPSL-
704 CM5 Earth System Model : From CMIP3 to CMIP5. *Climate Dynamics*, *40*(9‑10), 2123‑2165.
705 https://doi.org/10.1007/s00382-012-1636-1
706 Dulvy, N. K., Rogers, S. I., Jennings, S., Stelzenmller, V., Dye, S. R., & Skjoldal, H. R. (2008). Climate change
707 and deepening of the North Sea fish assemblage : A biotic indicator of warming seas. *Journal of*
708 *Applied Ecology*, *45*(4), 1029‑1039. https://doi.org/10.1111/j.1365-2664.2008.01488.x
709 Dunne, J. P., John, J. G., Adcroft, A. J., Griffies, S. M., Hallberg, R. W., Shevliakova, E., Stouffer, R. J., Cooke,
710 W., Dunne, K. A., Harrison, M. J., Krasting, J. P., Malyshev, S. L., Milly, P. C. D., Phillipps, P. J.,
711 Sentman, L. T., Samuels, B. L., Spelman, M. J., Winton, M., Wittenberg, A. T., & Zadeh, N. (2012).
712 GFDL's ESM2 Global Coupled Climate–Carbon Earth System Models. Part I : Physical Formulation
713 and Baseline Simulation Characteristics. *Journal of Climate*, *25*(19), 6646‑6665.
714 https://doi.org/10.1175/JCLI-D-11-00560.1
715 du Pontavice, H., Gascuel, D., Reygondeau, G., Maureaud, A., & Cheung, W. W. L. (2019). Climate change
716 undermines the global functioning of marine food webs. *Global Change Biology*, gcb.14944.
717 https://doi.org/10.1111/gcb.14944
718 Eddy, T. D., Bernhardt, J. R., Blanchard, J. L., Cheung, W. W. L., Colléter, M., du Pontavice, H., Fulton, E. A.,
719 Gascuel, D., Kearney, K. A., Petrik, C. M., Roy, T., Rykaczewski, R. R., Selden, R., Stock, C. A.,
720 Wabnitz, C. C. C., & Watson, R. A. (2021). Energy Flow Through Marine Ecosystems : Confronting

721 Transfer Efficiency. *Trends in Ecology & Evolution*, *36*(1), 76‑86.
722 https://doi.org/10.1016/j.tree.2020.09.006
723 Estes, J. A., Heithaus, M., McCauley, D. J., Rasher, D. B., & Worm, B. (2016). Megafaunal Impacts on
724 Structure and Function of Ocean Ecosystems. *Annual Review of Environment and Resources*, *41*(1),
725 83‑116. https://doi.org/10.1146/annurev-environ-110615-085622
726 Estes, J. A., Terborgh, J., Brashares, J. S., Power, M. E., Berger, J., Bond, W. J., Carpenter, S. R., Essington,
727 T. E., Holt, R. D., Jackson, J. B. C., Marquis, R. J., Oksanen, L., Oksanen, T., Paine, R. T., Pikitch, E. K.,
728 Ripple, W. J., Sandin, S. A., Scheffer, M., Schoener, T. W., … Wardle, D. A. (2011). Trophic
729 Downgrading of Planet Earth. *Science*, *333*(6040), 301‑306.
730 https://doi.org/10.1126/science.1205106
731 FAO (Éd.). (2018). *Meeting the sustainable development goals*.
732 Ferretti, F., Worm, B., Britten, G. L., Heithaus, M. R., & Lotze, H. K. (2010). Patterns and ecosystem
733 consequences of shark declines in the ocean : Ecosystem consequences of shark declines. *Ecology*
734 *Letters*, no-no. https://doi.org/10.1111/j.1461-0248.2010.01489.x
735 Friedland, K. D., Stock, C. A., Drinkwater, K. F., Link, J. S., Leaf, R. T., Shank, B. V., Rose, J. M., Pilskaln, C. H.,
736 & Fogarty, M. J. (2012). Pathways between Primary Production and Fisheries Yields of Large
737 Marine Ecosystems. *PLoS ONE*, *7*(1), e28945. https://doi.org/10.1371/journal.pone.0028945
738 Gasche, L., Gascuel, D., Shannon, L., & Shin, Y.-J. (2012). Global assessment of the fishing impacts on the
739 Southern Benguela ecosystem using an EcoTroph modelling approach. *Journal of Marine Systems*,
740 *90*(1), 1‑12. https://doi.org/10.1016/j.jmarsys.2011.07.012
741 Gascuel, D. (2005). The trophic-level based model : A theoretical approach of fishing effects on marine
742 ecosystems. *Ecological Modelling*, *189*(3‑4), 315‑332.
743 https://doi.org/10.1016/j.ecolmodel.2005.03.019

744 Gascuel, D., Bozec, Y., Chassot, E., Colomb, A., & Laurans, M. (2005). The trophic spectrum : Theory and
745 application as an ecosystem indicator. *ICES Journal of Marine Science*, *62*(3), 443‑452.
746 https://doi.org/10.1016/j.icesjms.2004.12.013
747 Gascuel, D., Guenette, S., & Pauly, D. (2011). The trophic-level-based ecosystem modelling approach :
748 Theoretical overview and practical uses. *ICES Journal of Marine Science*, *68*(7), 1403‑1416.
749 https://doi.org/10.1093/icesjms/fsr062
750 Gascuel, D., Morissette, L., Palomares, M. L. D., & Christensen, V. (2008). Trophic flow kinetics in marine
751 ecosystems : Toward a theoretical approach to ecosystem functioning. *Ecological Modelling*,
752 *217*(1‑2), 33‑47. https://doi.org/10.1016/j.ecolmodel.2008.05.012
753 Gascuel, D., & Pauly, D. (2009). EcoTroph : Modelling marine ecosystem functioning and impact of fishing.
754 *Ecological Modelling*, *220*(21), 2885‑2898. https://doi.org/10.1016/j.ecolmodel.2009.07.031
755 Giorgetta, M. A., Jungclaus, J., Reick, C. H., Legutke, S., Bader, J., Böttinger, M., Brovkin, V., Crueger, T.,
756 Esch, M., Fieg, K., Glushak, K., Gayler, V., Haak, H., Hollweg, H.-D., Ilyina, T., Kinne, S., Kornblueh,
757 L., Matei, D., Mauritsen, T., … Stevens, B. (2013). Climate and carbon cycle changes from 1850 to
758 2100 in MPI-ESM simulations for the Coupled Model Intercomparison Project phase 5 : Climate
759 Changes in MPI-ESM. *Journal of Advances in Modeling Earth Systems*, *5*(3), 572‑597.
760 https://doi.org/10.1002/jame.20038
761 Golden, C. D., Allison, E. H., Cheung, W. W. L., Dey, M. M., Halpern, B. S., McCauley, D. J., Smith, M., Vaitla,
762 B., Zeller, D., & Myers, S. S. (2016). Nutrition : Fall in fish catch threatens human health. *Nature*,
763 *534*(7607), 317‑320. https://doi.org/10.1038/534317a
764 Halouani, G., Gascuel, D., Hattab, T., Lasram, F. B. R., Coll, M., Tsagarakis, K., Piroddi, C., Romdhane, M. S.,
765 & Le Loc'h, F. (2015). Fishing impact in Mediterranean ecosystems : An EcoTroph modeling
766 approach. *Journal of Marine Systems*, *150*, 22‑33. https://doi.org/10.1016/j.jmarsys.2015.05.007

767 Heithaus, M. R., Frid, A., Wirsing, A. J., & Worm, B. (2008). Predicting ecological consequences of marine
768 top predator declines. *Trends in Ecology & Evolution*, *23*(4), 202-210.
769 https://doi.org/10.1016/j.tree.2008.01.003
770 Heneghan, R. F., Everett, J. D., Blanchard, J. L., & Richardson, A. J. (2016). Zooplankton Are Not Fish :
771 Improving Zooplankton Realism in Size-Spectrum Models Mediates Energy Transfer in Food Webs.
772 *Frontiers in Marine Science*, *3*. https://doi.org/10.3389/fmars.2016.00201
773 IPCC. (2014). *Climate Change 2014 : Synthesis Report. Contribution of Working Groups I, II and III to*
774 *the Fifth Assessment Report of the Intergovernmental Panel on Climate Change* (Core Writing
775 Team, R. K. Pachauri, & L. A. Meyer, Éds.). IPCC.
776 Irwin, A. J., Finkel, Z. V., Schofield, O. M. E., & Falkowski, P. G. (2006). Scaling-up from nutrient physiology
777 to the size-structure of phytoplankton communities. *Journal of Plankton Research*, *28*(5), 459-471.
778 https://doi.org/10.1093/plankt/fbi148
779 Jennings, S., & Collingridge, K. (2015). Predicting Consumer Biomass, Size-Structure, Production, Catch
780 Potential, Responses to Fishing and Associated Uncertainties in the World's Marine Ecosystems.
781 *PLOS ONE*, *10*(7), e0133794. https://doi.org/10.1371/journal.pone.0133794
782 Jones, M. C., & Cheung, W. W. L. (2015). Multi-model ensemble projections of climate change effects on
783 global marine biodiversity. *ICES Journal of Marine Science*, *72*(3), 741-752.
784 https://doi.org/10.1093/icesjms/fsu172
785 Kortsch, S., Primicerio, R., Aschan, M., Lind, S., Dolgov, A. V., & Planque, B. (2018). Food-web structure
786 varies along environmental gradients in a high-latitude marine ecosystem. *Ecography*.
787 https://doi.org/10.1111/ecog.03443
788 Kwiatkowski, L., Aumont, O., & Bopp, L. (2019). Consistent trophic amplification of marine biomass
789 declines under climate change. *Global Change Biology*, *25*(1), 218-229.
790 https://doi.org/10.1111/gcb.14468

791 Kwiatkowski, L., Bopp, L., Aumont, O., Ciais, P., Cox, P. M., Laufkötter, C., Li, Y., & Séférian, R. (2017).
792 Emergent constraints on projections of declining primary production in the tropical oceans. *Nature*
793 *Climate Change*, *7*(5), 355‑358. https://doi.org/10.1038/nclimate3265
794 Laufkötter, C., Vogt, M., Gruber, N., Aita-Noguchi, M., Aumont, O., Bopp, L., Buitenhuis, E., Doney, S. C.,
795 Dunne, J., Hashioka, T., Hauck, J., Hirata, T., John, J., Le Quéré, C., Lima, I. D., Nakano, H., Seferian,
796 R., Totterdell, I., Vichi, M., & Völker, C. (2015). Drivers and uncertainties of future global marine
797 primary production in marine ecosystem models. *Biogeosciences*, *12*(23), 6955‑6984.
798 https://doi.org/10.5194/bg-12-6955-2015
799 Longhurst, A. R. (2007). *Ecological geography of the sea* (2nd ed). Academic Press.
800 Lotze, H. K., Tittensor, D. P., Bryndum-Buchholz, A., Eddy, T. D., Cheung, W. W. L., Galbraith, E. D., Barange,
801 M., Barrier, N., Bianchi, D., Blanchard, J. L., Bopp, L., Büchner, M., Bulman, C. M., Carozza, D. A.,
802 Christensen, V., Coll, M., Dunne, J. P., Fulton, E. A., Jennings, S., … Worm, B. (2019). Global
803 ensemble projections reveal trophic amplification of ocean biomass declines with climate change.
804 *Proceedings of the National Academy of Sciences*, *116*(26), 12907‑12912.
805 https://doi.org/10.1073/pnas.1900194116
806 Maureaud, A., Gascuel, D., Colléter, M., Palomares, M. L. D., Du Pontavice, H., Pauly, D., & Cheung, W. W.
807 L. (2017). Global change in the trophic functioning of marine food webs. *PLOS ONE*, *12*(8),
808 e0182826. https://doi.org/10.1371/journal.pone.0182826
809 Montero-Serra, I., Edwards, M., & Genner, M. J. (2015). Warming shelf seas drive the subtropicalization of
810 European pelagic fish communities. *Global Change Biology*, *21*(1), 144‑153.
811 https://doi.org/10.1111/gcb.12747
812 Morán, X. A. G., López-Urrutia, Á., Calvo-Díaz, A., & Li, W. K. W. (2010). Increasing importance of small
813 phytoplankton in a warmer ocean. *Global Change Biology*, *16*(3), 1137‑1144.
814 https://doi.org/10.1111/j.1365-2486.2009.01960.x

Pauly, D. (1998). Fishing Down Marine Food Webs. *Science*, *279*(5352), 860-863. https://doi.org/10.1126/science.279.5352.860

Petrik, C. M., Stock, C. A., Andersen, K. H., van Denderen, P. D., & Watson, J. R. (2019). Bottom-up drivers of global patterns of demersal, forage, and pelagic fishes. *Progress in Oceanography*, *176*, 102124. https://doi.org/10.1016/j.pocean.2019.102124

Petrik, C. M., Stock, C. A., Andersen, K. H., van Denderen, P. D., & Watson, J. R. (2020). Large Pelagic Fish Are Most Sensitive to Climate Change Despite Pelagification of Ocean Food Webs. *Frontiers in Marine Science*, *7*, 588482. https://doi.org/10.3389/fmars.2020.588482

Pinsky, M. L., Worm, B., Fogarty, M. J., Sarmiento, J. L., & Levin, S. A. (2013). Marine Taxa Track Local Climate Velocities. *Science*, *341*(6151), 1239-1242. https://doi.org/10.1126/science.1239352

Poloczanska, E. S., Brown, C. J., Sydeman, W. J., Kiessling, W., Schoeman, D. S., Moore, P. J., Brander, K., Bruno, J. F., Buckley, L. B., Burrows, M. T., Duarte, C. M., Halpern, B. S., Holding, J., Kappel, C. V., O'Connor, M. I., Pandolfi, J. M., Parmesan, C., Schwing, F., Thompson, S. A., & Richardson, A. J. (2013). Global imprint of climate change on marine life. *Nature Climate Change*, *3*(10), 919-925. https://doi.org/10.1038/nclimate1958

Pörtner, H. O., Bock, C., & Mark, F. C. (2017). Oxygen- and capacity-limited thermal tolerance : Bridging ecology and physiology. *The Journal of Experimental Biology*, *220*(15), 2685-2696. https://doi.org/10.1242/jeb.134585

Pörtner, H. O., & Farrell, A. P. (2008). ECOLOGY : Physiology and Climate Change. *Science*, *322*(5902), 690-692. https://doi.org/10.1126/science.1163156

Pörtner, H. O., & Peck, M. A. (2010). Climate change effects on fishes and fisheries : Towards a cause-and-effect understanding. *Journal of Fish Biology*, *77*(8), 1745-1779. https://doi.org/10.1111/j.1095-8649.2010.02783.x

838 Rasher, D. B., Steneck, R. S., Halfar, J., Kroeker, K. J., Ries, J. B., Tinker, M. T., Chan, P. T. W., Fietzke, J.,
839 Kamenos, N. A., Konar, B. H., Lefcheck, J. S., Norley, C. J. D., Weitzman, B. P., Westfield, I. T., &
840 Estes, J. A. (2020). Keystone predators govern the pathway and pace of climate impacts in a
841 subarctic marine ecosystem. *Science*, *369*(6509), 1351‑1354.
842 https://doi.org/10.1126/science.aav7515
843 Reygondeau, G., Longhurst, A., Martinez, E., Beaugrand, G., Antoine, D., & Maury, O. (2013). Dynamic
844 biogeochemical provinces in the global ocean : DYNAMIC BIOGEOCHEMICAL PROVINCES. *Global*
845 *Biogeochemical Cycles*, *27*(4), 1046‑1058. https://doi.org/10.1002/gbc.20089
846 Ryther, J. H. (1969). Photosynthesis and Fish Production in the Sea. *Science*, *166*(3901), 72‑76.
847 https://doi.org/10.1126/science.166.3901.72
848 Steinacher, M., Joos, F., Frolicher, T. L., Bopp, L., Cadule, P., Cocco, V., Doney, S. C., Gehlen, M., Lindsay,
849 K., Moore, J. K., Schneider, B., & Segschneider, J. (2010). *Projected 21st century decrease in marine*
850 *productivity : A multi-model analysis*. 27.
851 Stock, C. A., & Dunne, J. (2010). Controls on the ratio of mesozooplankton production to primary
852 production in marine ecosystems. *Deep Sea Research Part I: Oceanographic Research Papers*,
853 *57*(1), 95‑112. https://doi.org/10.1016/j.dsr.2009.10.006
854 Stock, C. A., Dunne, J. P., & John, J. G. (2014a). Global-scale carbon and energy flows through the marine
855 planktonic food web : An analysis with a coupled physical–biological model. *Progress in*
856 *Oceanography*, *120*, 1‑28. https://doi.org/10.1016/j.pocean.2013.07.001
857 Stock, C. A., Dunne, J. P., & John, J. G. (2014b). Drivers of trophic amplification of ocean productivity trends
858 in a changing climate. *Biogeosciences*, *11*(24), 7125‑7135. https://doi.org/10.5194/bg-11-7125-
859 2014
860 Stock, C. A., John, J. G., Rykaczewski, R. R., Asch, R. G., Cheung, W. W. L., Dunne, J. P., Friedland, K. D., Lam,
861 V. W. Y., Sarmiento, J. L., & Watson, R. A. (2017). Reconciling fisheries catch and ocean

productivity. *Proceedings of the National Academy of Sciences of the United States of America*, *114*(8), E1441-E1449. https://doi.org/10.1073/pnas.1610238114

Thackeray, S. J., Henrys, P. A., Hemming, D., Bell, J. R., Botham, M. S., Burthe, S., Helaouet, P., Johns, D. G., Jones, I. D., Leech, D. I., Mackay, E. B., Massimino, D., Atkinson, S., Bacon, P. J., Brereton, T. M., Carvalho, L., Clutton-Brock, T. H., Duck, C., Edwards, M., … Wanless, S. (2016). Phenological sensitivity to climate across taxa and trophic levels. *Nature*, *535*(7611), 241-245. https://doi.org/10.1038/nature18608

Vancoppenolle, M., Bopp, L., Madec, G., Dunne, J., Ilyina, T., Halloran, P. R., & Steiner, N. (2013). Future Arctic Ocean primary productivity from CMIP5 simulations : Uncertain outcome, but consistent mechanisms: FUTURE ARCTIC OCEAN PRIMARY PRODUCTIVITY. *Global Biogeochemical Cycles*, *27*(3), 605-619. https://doi.org/10.1002/gbc.20055

Verges, A., Steinberg, P. D., Hay, M. E., Poore, A. G. B., Campbell, A. H., Ballesteros, E., Heck, K. L., Booth, D. J., Coleman, M. A., Feary, D. A., Figueira, W., Langlois, T., Marzinelli, E. M., Mizerek, T., Mumby, P. J., Nakamura, Y., Roughan, M., van Sebille, E., Gupta, A. S., … Wilson, S. K. (2014). The tropicalization of temperate marine ecosystems : Climate-mediated changes in herbivory and community phase shifts. *Proceedings of the Royal Society B: Biological Sciences*, *281*(1789), 20140846-20140846. https://doi.org/10.1098/rspb.2014.0846

Woodland, R. J., & Secor, D. H. (2013). Benthic-pelagic coupling in a temperate inner continental shelf fish assemblage. *Limnology and Oceanography*, *58*(3), 966-976. https://doi.org/10.4319/lo.2013.58.3.0966

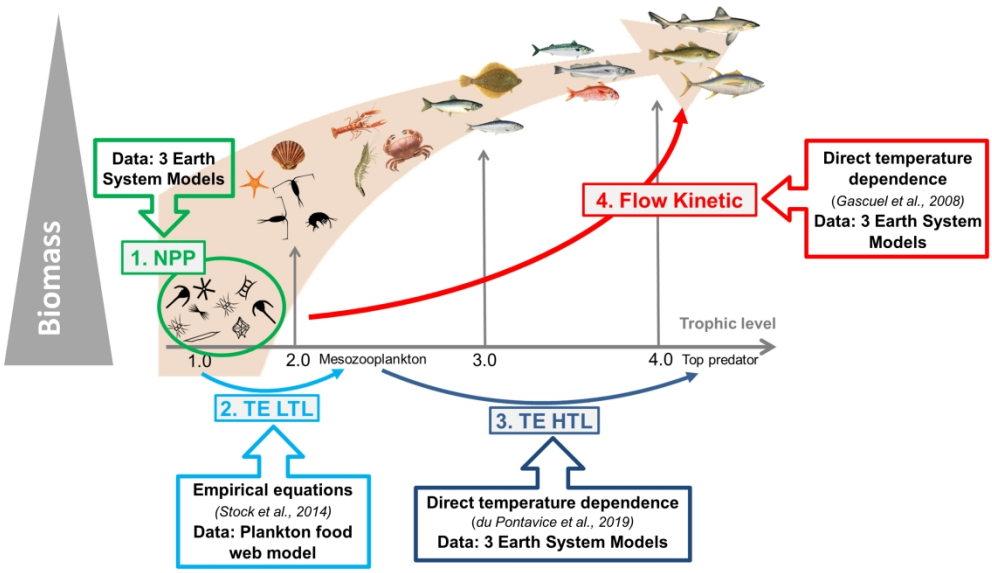

Figure 1: Conceptual design of the EcoTroph model and forcing used. The trophic functioning of marine food webs is represented by a biomass flow, with biomass entering the system at trophic level 1 due to net primary production, NPP. Biomass flow reaching each trophic level is then defined by the trophic transfer efficiency at low and high trophic level, TE LTL (derived from the plankton food web model COBALT) and TE HTL (estimated from the sea surface temperature (SST) according to du Pontavice et al. (2019)), respectively. The flow kinetics, which is also forced by SST (Gascuel et al., 2008), is a key parameter to derive biomass at each trophic level of the model from the biomass flow (Gascuel & Pauly, 2009). One EcoTroph model is implemented each year within each cell of the global ocean, forced by NPP and SST from Earth system models' projections.

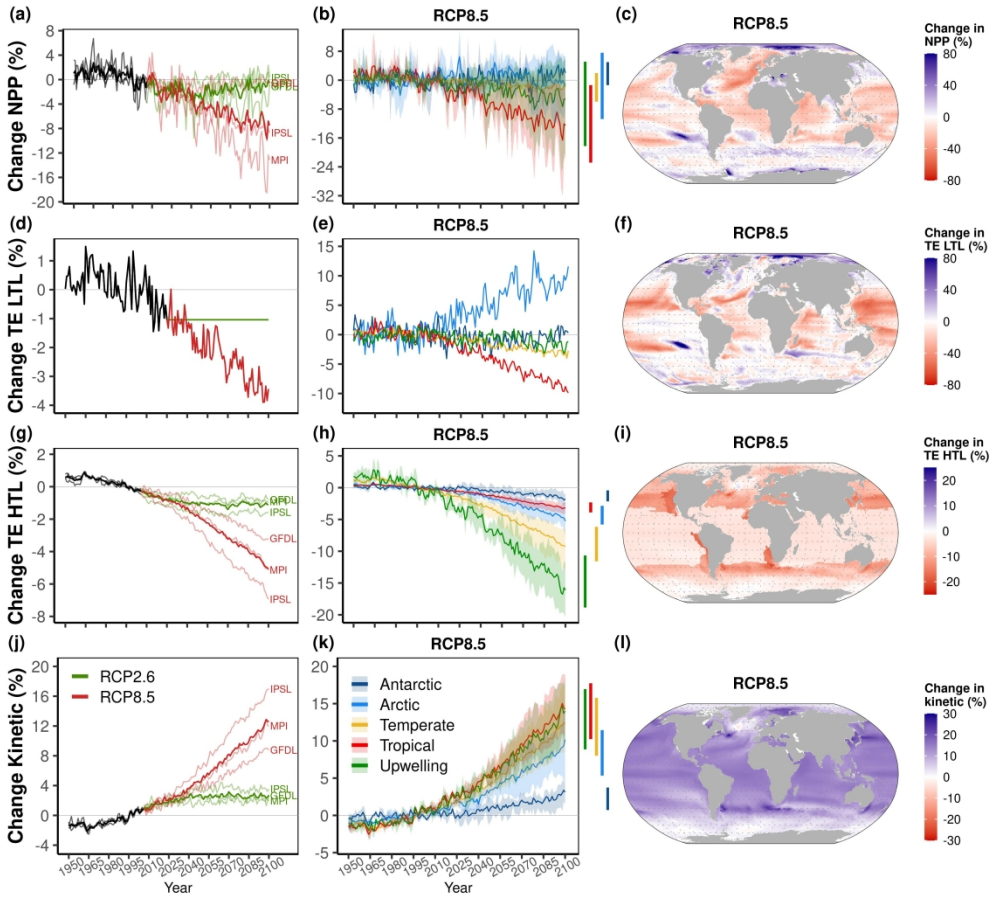

FIGURE 2: Projected changes in biomass flow processes between 1950 and 2100 relative to 1986–2005. The changes in net primary production, NPP, (a, b, c), transfer efficiency of low trophic levels, TE LTL, (d, e, f), transfer efficiency of higher trophic levels, TE HTL, (g, h, i) and flow kinetic (j, k, l) are represented on this figure. Panels (a), (d), (g) and (j) represent the changes at global scale for RCP2.6 and RCP8.5. Panels (b), (e), (h) and (k) represent the changes in each ecosystem type under RCP8.5. The shaded areas around the curves in these panels indicate the inter-model variability (i.e., the variability given by the inputs of the 3 different Earth system models) and the color bars outside the box indicate the range of averaged changes of the three Earth system models over 2090–2099. Panels (c), (f), (i) and (l) represent the changes over the period 2090–2099 in each 1°x1° grid cell.

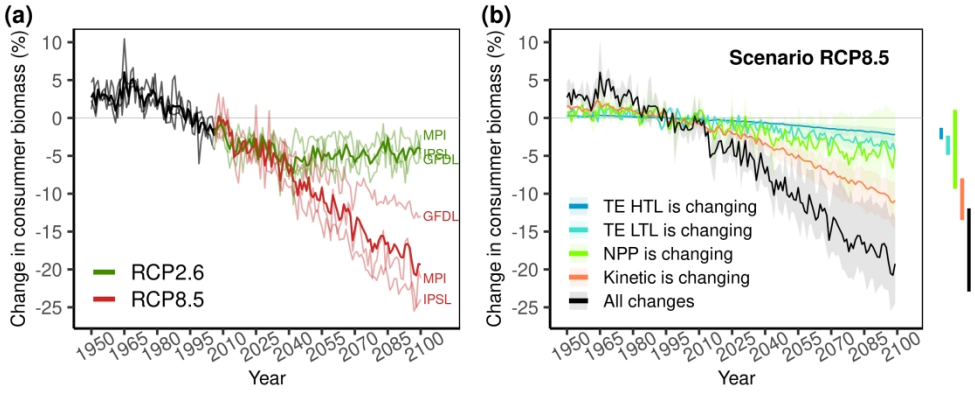

FIGURE 3: Changes in total consumer biomass over the period 1950–2100. (a) Changes in total consumer biomass for RCP2.6 and RCP8.5 relative to the reference period 1986–2005. (b) Mean changes in total consumer biomass for RCP8.5 relative to 1986–2005 in which the contribution of net primary production (NPP), transfer efficiency of lower trophic level (TE LTL), transfer efficiency of higher trophic level (TE HTL) and flow kinetic are isolated. The shaded areas around the curves indicate the inter-model variability and the color bars indicate the ranges of averaged changes of three Earth system models over 2090–2099.

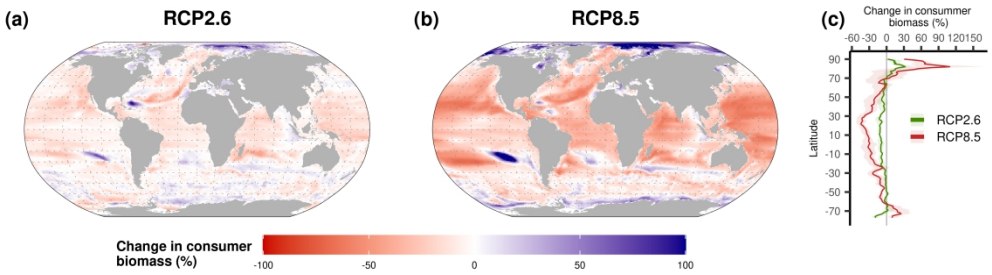

FIGURE 4: Maps of the ensemble mean projections for the three Earth system models of changes in total consumer biomass by 2090–2099 relative to 1986–2005 under (a) RCP2.6 and (b) RCP8.5. Panel (c) represents the changes in consumer biomass by latitude for RCP2.6 and RCP8.5.

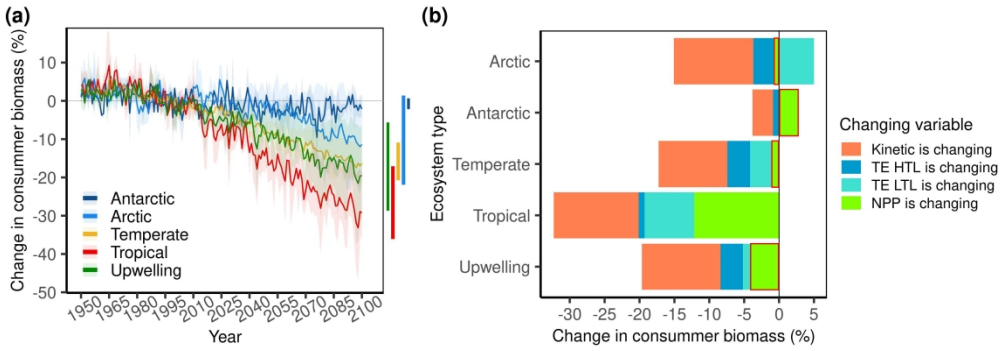

FIGURE 5: Changes in total consumer biomass in each ecosystem type as well as the processes at play for RCP8.5. Panel (a) represents the changes in total consumer biomass for RCP8.5 in each ecosystem type relative to the reference period 1986–2005. Panel (b) represents the mean contribution of the four processes in each ecosystem type (net primary production (NPP), transfer efficiency of lower trophic level (TE LTL), transfer efficiency of higher trophic level (TE HTL) and flow kinetic). The contribution is framed in red color if biomass projections with one of the three models predicts changes in the opposite direction to those predict with the two other models.

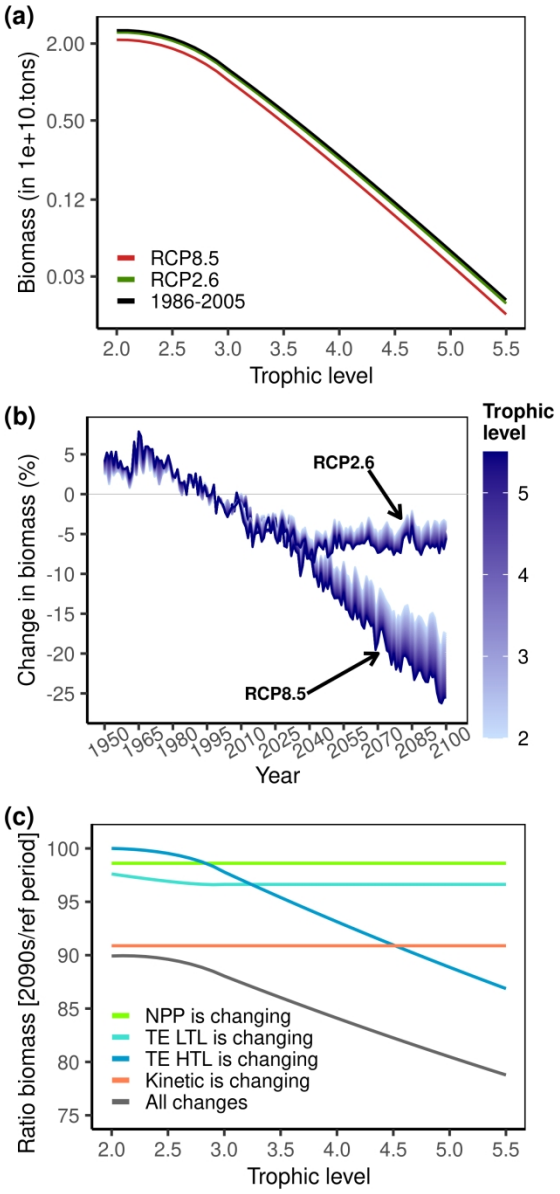

FIGURE 6: Changes in trophic structure under RCP2.6 and 8.5. (a) Biomass trophic spectra for RCP2.6 and RCP8.5 in 2090–2099 and the reference period in 1986–2005, while (b) Changes in biomass for each trophic class of width 0.1 trophic level (TL) between TL = 2 and TL = 5.5 under RCP2.6 and RCP8.5 relative to the reference period 1986–2005. (c) The ratio of biomass trophic spectra in 2090–2099 for RCP8.5 and for the reference period 1986–2005 derived from EcoTroph projections in which each flow parameter is successively isolated (net primary production (NPP), transfer efficiency of lower trophic level (TE LTL), transfer efficiency of higher trophic level (TE HTL) and flow kinetic).

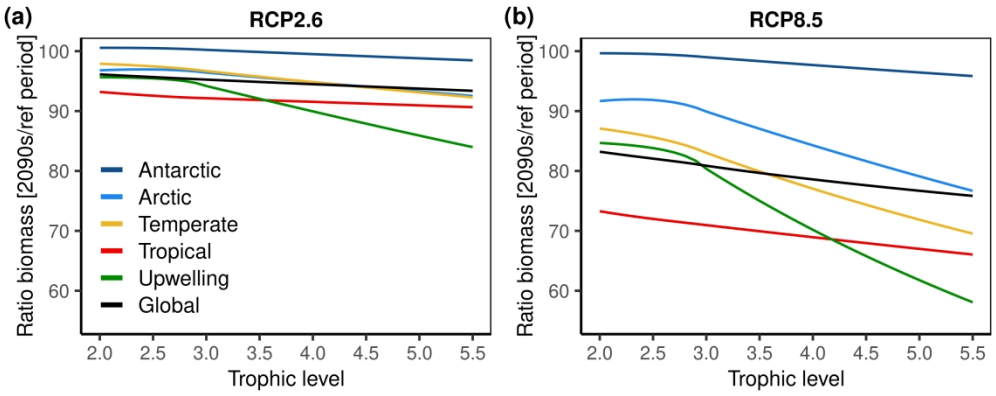

FIGURE 7: Changes in trophic structure in each ecosystem type for RCP2.6 and 8.5. The two panels show the ratio of the biomass spectrum in 2090-2090 to the reference period 1986–2005 for RCP2.6 (a) and RCP8.5 (b) for each ecosystem type.

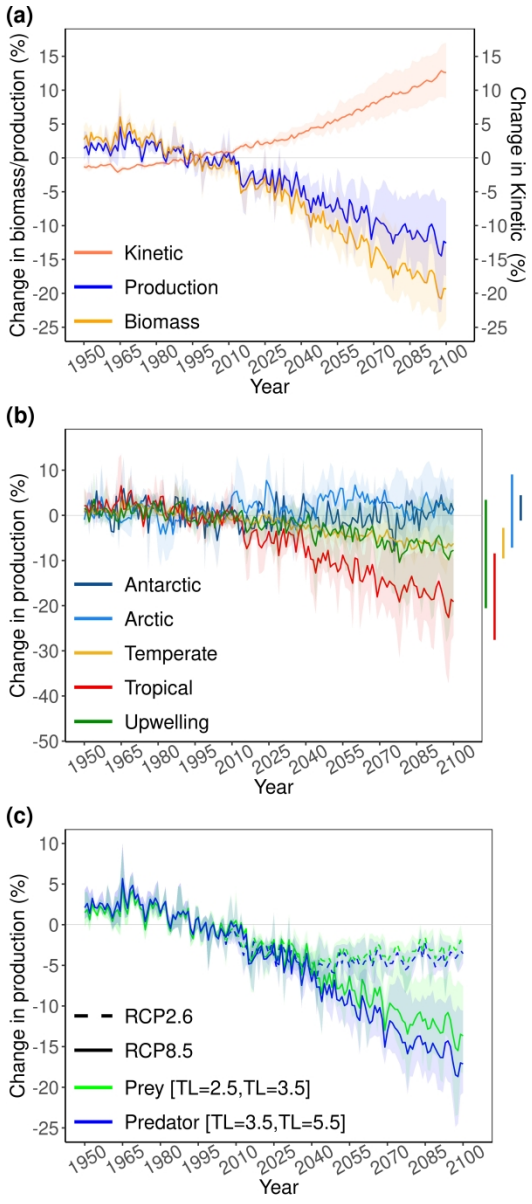

FIGURE 8: Changes in production at global scale and in each ecosystem type over the 21st century. Panel (a) represents the changes in total consumer production and biomass and in kinetic under RCP8.5 by 2100 relative to the reference period 1986–2005 while panel (b) represents the changes in total consumer production for RCP8.5 in each ecosystem type. Panel (c) represents the changes in prey (between trophic level (TL) = 2.5 and TL = 3.5) and predator (up to TL = 3.5) under RCP2.6 and RCP8.5.